Electronic Supplementary Material (ESI) for *Chemical Communications*
This journal is (c) The Royal Society of Chemistry 2015

Electronic Supplementary Information

Microwave *vs* solvothermal synthesis of hollow cobalt sulfide nanoprisms for electrocatalytic hydrogen evolution and supercapacitor

Bo You,† Nan Jiang,† Meili Sheng and Yujie Sun*
Department of Chemistry and Biochemistry, Utah State University, Logan, Utah 84322-0300, USA E-mail: yujie.sun@usu.edu; *Fax: +1-435-797-3390; Tel: +1-435-797-7608*

† These authors contributed equally

I. Experimental details

1. Chemicals

Polyvinylpyrrolidone (PVP, PVP10, MW ~ 10000) was purchased from TCI. Thioacetamide (TAA) was purchased from Alfa Aesar. Cobalt acetate tetrahydrate, Nafion, monobasic dihydrogen phosphate, and dibasic onohydrogen phosphate were purchased from Sigma-Aldrich. Ethanol was purchased from DECON LABORATORIES. All chemicals were used as received without any further purification. Water deionized (18 ohm) with a Barnstead E-Pure system was used in all experiments.

2. Microwave-assisted synthesis of the cobalt acetate hydroxide precursors (CAHs)

In a typical preparation, 2.25 g polyvinylpyrrolidone (PVP, PVP10, MW ~ 10000) and 0.96 g cobalt acetate tetrahydrate were dissolved in 150 ml ethanol at room temperature to afford a clear pink solution. Next, the resulting pink solution was subjected to microwave-treatment at 85 ℃ for 10 min. After centrifugation and rinsing with ethanol and drying, the cobalt acetate hydroxide precursors (CAHs) were obtained.

3. Synthesis of the hollow cobalt sulfide nanoprisms via microwave (MW-CoS) and solvothermal (ST-CoS) methods

For the formation of MW-CoS, 0.080 g cobalt acetate hydroxide precursors (CAHs) and 0.1125 g thioacetamide (TAA) were dispersed into 40 mL ethanol. The resulting mixture was subjected to microwave treatment at 120 ℃ for 5 min or solvothermal treatment at 120 ℃ for 6 h to obtain MW-CoS or ST-CoS, respectively.

4. Physical Methods

Scanning electron microscopy (SEM) and transmission electron microscopy (TEM) measurements were collected on a FEI QUANTA FEG 650 (FEI, USA). X-ray diffraction (XRD) patterns were recorded on a Rigaku MinifexII Desktop X-ray diffractometer. Nitrogen sorption isotherms were measured at 77 K with an autosorb iQ automated gas sorption analyzer (Quantachrome Instruments, USA). Before measurements, the samples were degassed in a vacuum at 200 ℃ for at least 5 h. The Brunauer-Emmett-Teller (BET) method and the Barrett-Joyner-Halenda (BJH) model were utilized to calculate the specific surface area (BET), pore volume and pore size distribution, respectively. The total pore volumes (V_t) were estimated from the adsorbed amount of nitrogen at a relative pressure P/P_0 of 0.995. The X-ray photoelectron spectroscopy analyses were performed using a Kratos Axis Ultra instrument (Chestnut Ridge, NY) at the Surface Analysis Laboratory, University of Utah Nanofab. The samples were affixed on a stainless steel Kratos sample bar, loaded into the instrument's load lock chamber, and evacuated to 5×10^{-8} torr before it was transferred into the sample analysis chamber under ultrahigh vacuum conditions (~10^{-10} torr). X-ray photoelectron spectra were collected using the monochromatic Al Kα source (1486.7 eV) at a 300 × 700 μm spot size. Low resolution survey and high resolution region scans at the binding energy of interest were collected for each sample. To minimize charging, all samples were flooded with low-energy electrons and ions from the instrument's built-in charge neutralizer. The samples were also sputter cleaned inside the analysis chamber with 1 keV Ar^+ ions for 30 seconds to remove adventitious contaminants and surface oxides. XPS data were analyzed using CASA XPS software, and energy corrections on high resolution scans were calibrated by referencing the C 1s peak of adventitious carbon to 284.5 eV. The generated hydrogen volume during electrolysis was quantified with a SRI gas chromatography system 8610C equipped with a molecular sieve 13× packed column, a HayesSep D packed column, and a thermal conductivity detector. The oven temperature was maintained at 60 °C and argon was used as the carrier gas.

5. Electrochemical measurements

5.1 Electrocatalytic hydrogen evolution

The resulted samples ink (MW-CoS or ST-CoS) was prepared by ultrasonically mixing 4 mg of the catalyst powder with the mixture of 1160 μL ethanol, 800 μL H_2O and 40 μL 5 % Nafion solution for 20 min to form a homogeneous catalyst ink. Then, 10 μL of the catalyst ink was carefully dropped onto the polished glassy carbon rotating disk electrode (RDE), leading to the catalyst loading of 0.283 mg cm^{-2}.

Electrochemical measurements of cyclic voltammetry were performed by a computer-controlled Gamry Interface 1000 electrochemical workstation with a three-electrode cell system. A glass carbon RDE (RRDE-3A, d = 3 mm, S = 0.07065 cm^2) coated with the catalyst ink was used as the working electrode, a Ag/AgCl (sat. KCl) electrode as the reference electrode, and a Pt wire as the counter electrode. The electrochemical experiments were conducted in N_2 saturated 1.0 M pH 7 phosphate buffer or 1.0 M KOH electrolyte for the hydrogen evolution reaction at room temperature. The potential range is cyclically scanned from open-circuit voltage to –1.1 V vs. Ag/AgCl (for 1.0 M pH 7 phosphate buffer) or –1.4 V vs. Ag/AgCl (for 1.0 M KOH) at a scan rate of 2 mV s^{-1} and a rotating speed of 2000 rpm. Electric impedance spectroscopy measurements in N_2 saturated 1.0 M pH 7 phosphate buffer were carried out in the same configuration at -0.650 V vs. SHE from 10^5 to 0.1 Hz with an AC potential amplitude of 30 mV. All potentials reported in HER testing were converted from vs. Ag/AgCl to vs. SHE by adding 0.197 V. The reference electrode in neutral aqueous media was calibrated with ferrocenecarboxylic acid whose $Fe^{3+/2+}$ couple is 0.284 V vs. SCE.[S1] iR (current times internal resistance) compensation was applied in polarization and controlled potential electrolysis experiments to account for the voltage drop between the reference and working electrodes using Gamry Framework™ Data Acquisition Software 6.11.

The durability of the samples in neutral water and 1.0 M KOH was assessed via long-term controlled potential electrolysis at –0.650 V vs SHE for 21 h and –1.060 V vs SHE for 5.5 h, respectively.

5.2 Evaluation of the supercapacitor properties

The supercapacitor properties of the prepared samples were investigated with a CHI 760E electrochemical workstation (CH Instruments) in 1 M KOH using cyclic voltammetry (CV), galvanostatic charge/discharge (GV) in a conventional three-electrode cell at various scan rates and current densities, respectively. The catalyst-loaded glassy carbon electrode with a mass loading of 1 mg cm^{-2} was directly used as the working electrode. A Ag/AgCl (sat. KCl) and a Pt wire were used as the reference and counter electrodes, respectively. Specific capacitances derived from galvanostatic (GV) tests can be calculated from the equation:

$$C = I\Delta t/m\Delta V$$

where C ($F\ g^{-1}$), I (A), Δt (s), m (g) and ΔV are the specific capacitance, the discharge current, the discharge time, the mass of the active materials in electrode, and the potential window, respectively.

II. Supplementary Results

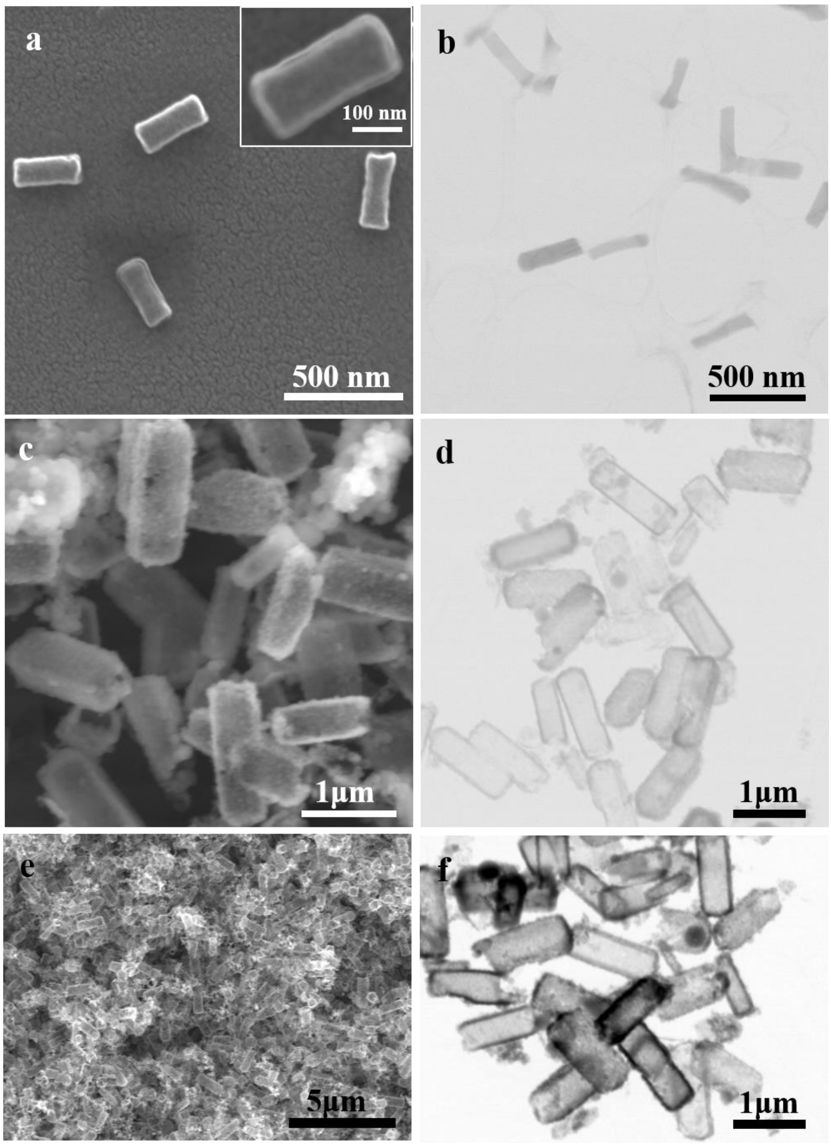

Fig. S1 SEM (a, c and e) and TEM (b, d and f) images of cobalt acetate hydroxide precursor (a and b), ST-CoS (c and d), and MW-CoS (e and f).

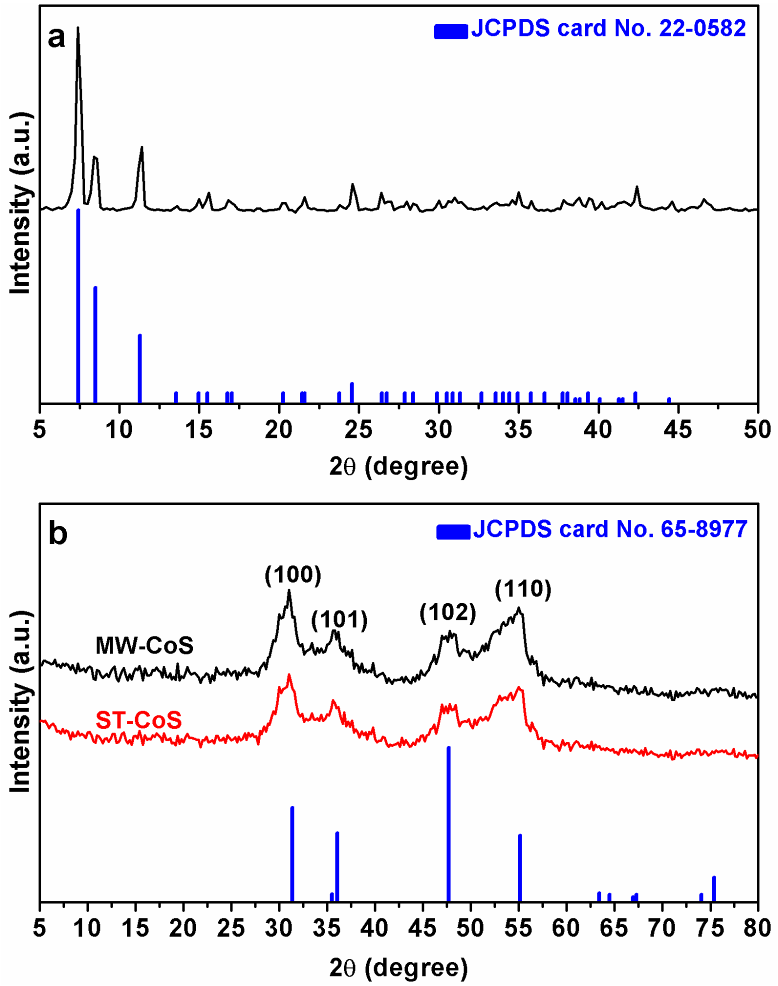

Fig. S2 XRD patterns of (a) cobalt acetate hydroxide precursor and (b) MW-CoS and ST-CoS.

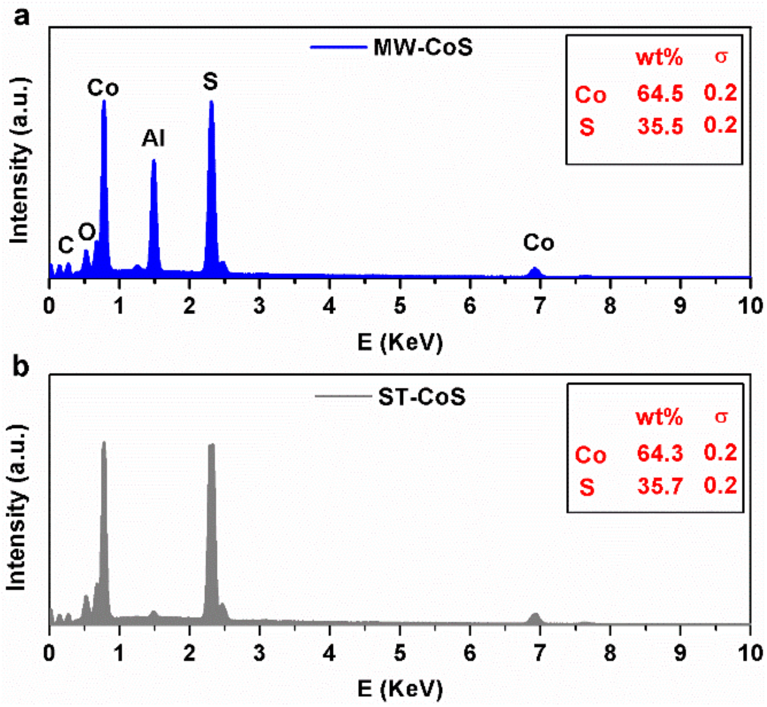

Fig. S3 EDX of (a) MW-CoS and (b) ST-CoS. The Al peak is due to the substrate.

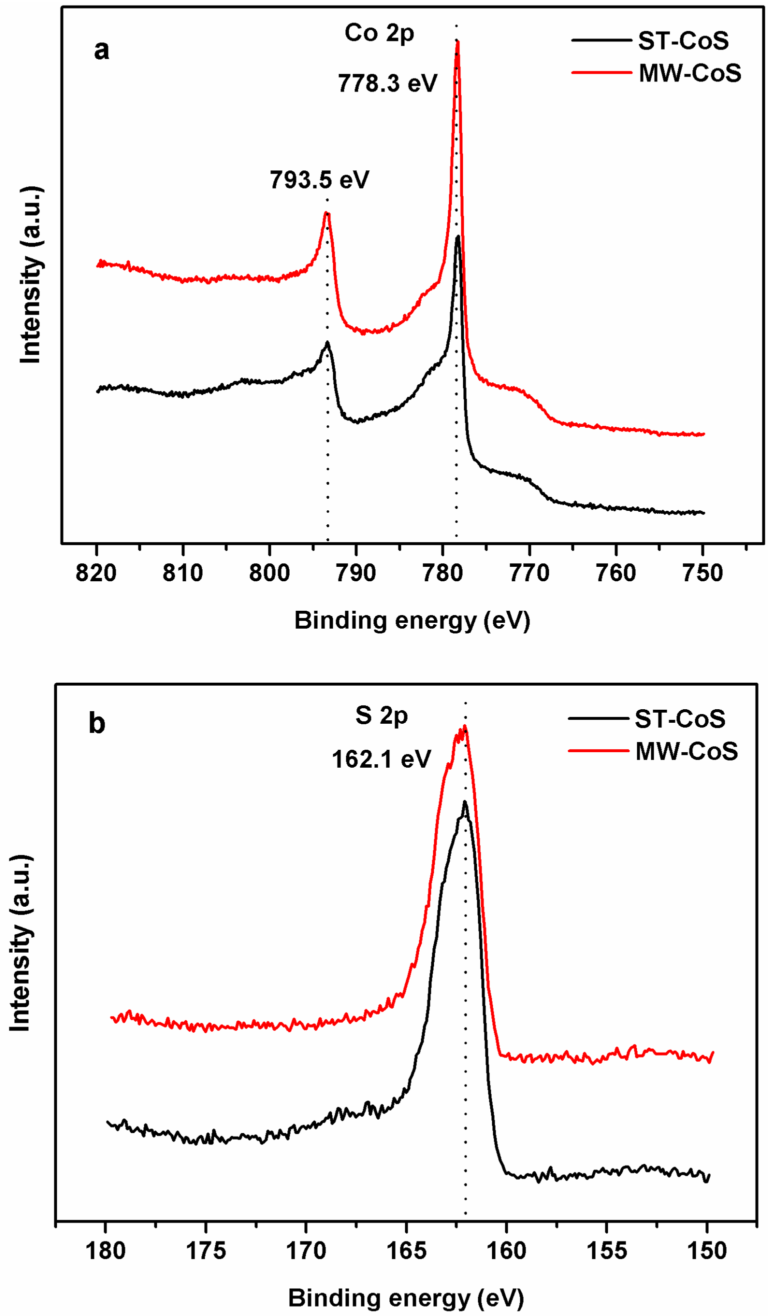

Fig. S4 XPS spectra of (a) Co 2p and (b) S 2p for MW-CoS and ST-CoS.

Table S1. Comparison of HER performance in neutral media for MW-CoS with other HER electrocatalysts.

Catalysts	**Loading**	**Electrolyte**	**Tafel slope (mV dec^{-1})**	**η_1 ^{a} (mV)**	**η_{10} ^{a} (mV)**	**References**
MW-CoS	0.283 mg cm^{-2}	1.0 M KPi	75	198	275	**This work**
H_2-CoCat/FTO	Co=58.9 μg cm^{-2}	0.5 M KPi	140	~325	-	*Nat. Mater.*, **2012**, 11, 802.
CoP/CC	0.92 mg cm^{-2}	1.0 M KPi	93	~60	~200	*J. Am. Chem. Soc.*, **2014**, 136, 7587.
Co-NRCNT	0.280 mg cm^{-2}	0.1 M KPi		330	540	*Angew. Chem. Int. Ed.*, **2014**, 53, 4372
Cu_2MoS_4	0.042 mg cm^{-2}	0.1 M KPi	95	~200	~350	*Energy Environ. Sci.*, **2012**, 5, 8912
Mo_2B	~339 mg cm^{-2}	1.0 M KPi	-	250	-	*Angew. Chem. Int. Ed.*, **2012**, 51, 12703
Mo_2C	~339 mg cm^{-2}	1.0 M KPi	-	200	-	*Angew. Chem. Int. Ed.*, **2012**, 51, 12703
H_2-NiCat film	-	0.1 M NaBi	226	~250	>600	*J. Phys. Chem. C*, **2014**, 118, 4578.
Ni-S film	Ni=81.5 μg cm^{-2}	1.0 M KPi	77	227	330	*J. Mater. Chem. A*, **2014**, 2, 19407.
$Fe_{1-x}S$	2.128 mg cm^{-2}	0.1 M KPi	150	>637	-	*ACS Catal.* **2014**, 4, 681.

^{a} Overpotential required to reach current densities of 1 or 10 mA cm^{-2}.

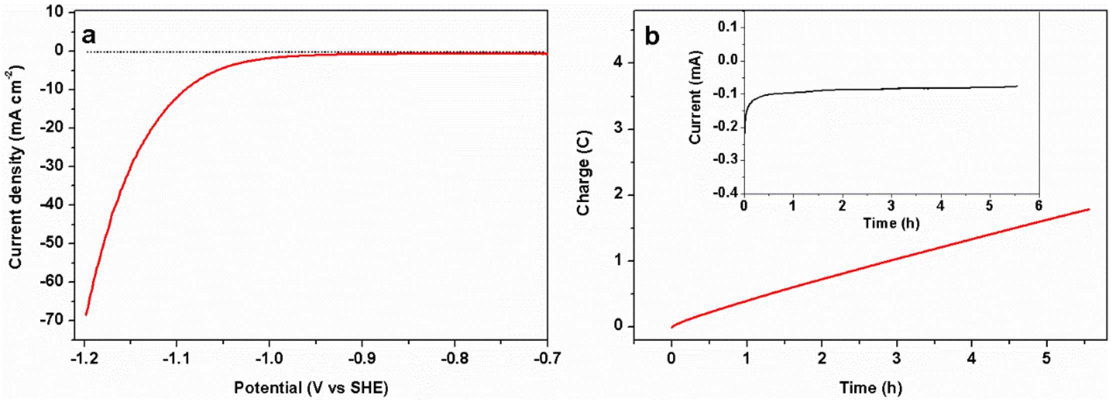

Fig. S5 (a) Polarization curves of MW-CoS at 2 mV s^{-1} and 2000 rpm in 1 M KOH. (b) Long-term controlled potential electrolysis of MW-CoS. Then inset in (b) is the corresponding current change over time during the electrolysis experiments.

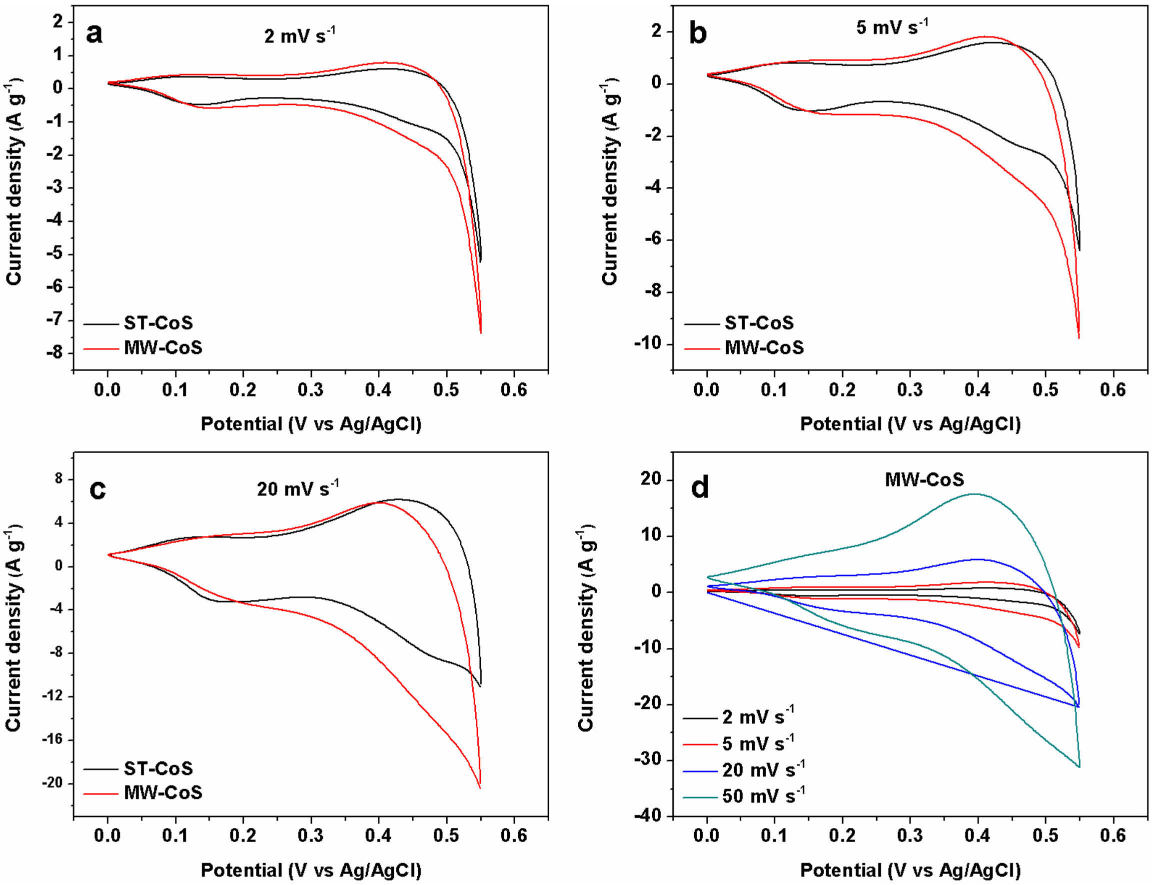

Fig. S6 (a-c) Cyclic voltammetry curves of ST-CoS and MW-CoS at scan rate of 2, 5 and 20 mV s^{-1}. (d) Cyclic voltammetry curves of MW-CoS at different scan rate.

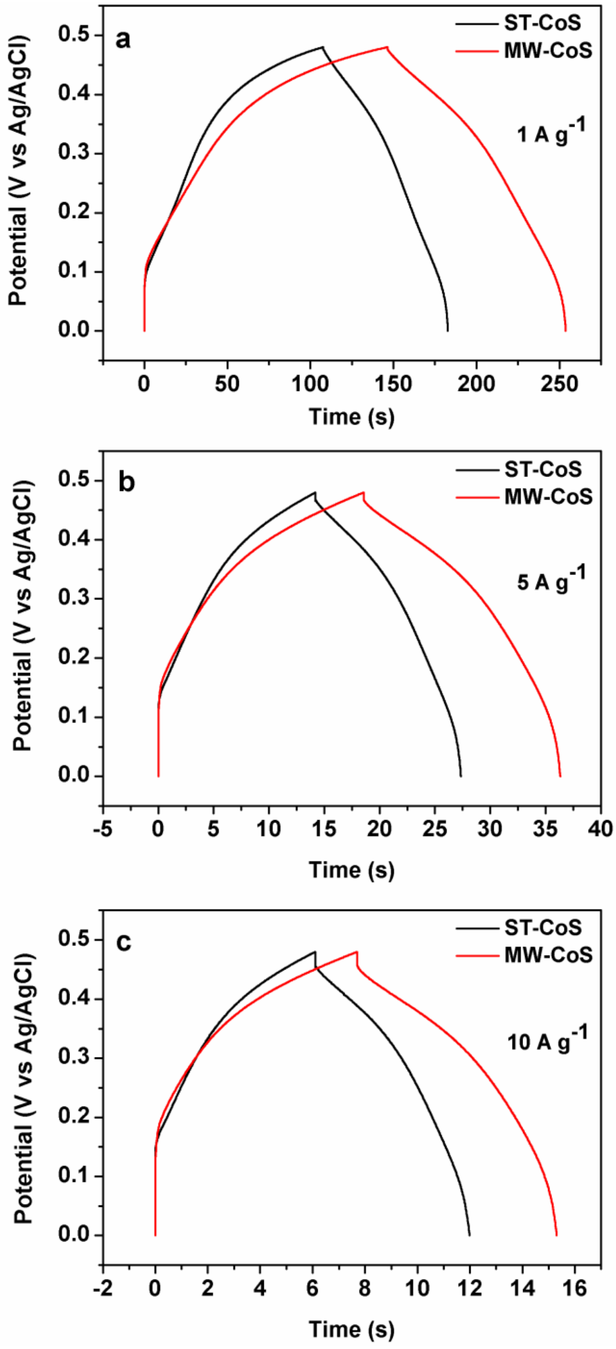

Fig. S7 Galvanostatic charge-discharge curves of MW-CoS and ST-CoS samples at current density of (a) 1 A g^{-1}, (b) 5 A g^{-1} and (c) 10 A g^{-1}.

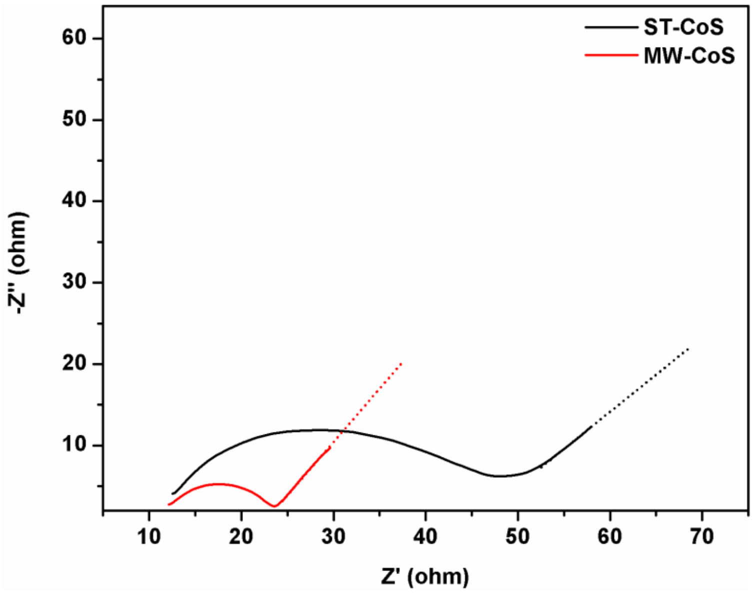

Fig. S8 Nyquist plots of MW-CoS- and ST-CoS-based supercapacitor electrode

Both of the Nyquist plots show a straight line in the low frequency region and an arc in the high frequency region. At high frequency (close to 100 kHz), the intercept with the Z’ axis (real impedance axis) represents the intrinsic Ohmic resistance of the internal resistance or equivalent series resistance (ESR) of the electrode material and electrolyte.[S2] As shown in Fig. S7, both electrodes show a similar value (12 ohm), demonstrating similar electrical resistance. At moderate frequency, the MW-CoS electrode shows an arc with smaller semicircular diameter compared to that of ST-CoS, implying faster charge transfer. Moreover, at low frequency, the slope of the linear plots reflects the diffusive resistivity of the electrolyte ions within the pores. A steeper gradient corresponds to faster ion diffusion. Clearly, the slope for MW-CoS electrode is larger than that of ST-CoS electrode, suggesting faster ion diffusion behavior. This is because the larger porosities together with higher specific surface area of MW-CoS could buffer electrolytes to reduce ion transport resistance and minimize ion diffusion distance and facilitate ion transport.

Supplementary References

[S1] E. Liaudet, F. Battaglini and E. J. Calvo, *J. Electroanal. Chem. Interfacial Electrochem.*, 1990, **293**, 55.

[S2] B. G. Choi, J. Hong, W. H. Hong, P. T. Hammond and H. Park, *ACS Nano*, 2011, **5**, 7205.